Implications of the Top Quark Mass Measurement for the CKM Parameters, x_s and CP Asymmetries (Revised and Updated)

A. Ali[*]

Theory Division, CERN
CH-1211 Geneva 23, Switzerland

and

D. London

Laboratoire de physique nucléaire, Université de Montréal
C.P. 6128, succ. centre-ville, Montréal, QC, Canada H3C 3J7

Abstract

Motivated by the recent determination of the top quark mass by the CDF collaboration, $m_t = 174 \pm 10^{+13}_{-12}$ GeV, we review and update the constraints on the parameters of the quark flavour mixing matrix V_{CKM} in the standard model. In performing our fits, we use inputs from the measurements of the following quantities: (i) $|\epsilon|$, the CP-violating parameter in K decays, (ii) ΔM_d, the mass difference due to the B_d^0-$\overline{B_d^0}$ mixing, (iii) the matrix elements $|V_{cb}|$ and $|V_{ub}|$, and (iv) B-hadron lifetimes. We find that the allowed region of the unitarity triangle is very large, mostly due to theoretical uncertainties. (This emphasizes the importance of measurements of CP-violating rate asymmetries in the B system.) Nevertheless, the present data do somewhat restrict the allowed values of the coupling constant product $f_{B_d}\sqrt{\hat{B}_{B_d}}$ and the renormalization-scale-invariant bag constant $\hat{B}_K$. With the updated CKM matrix we present the currently-allowed range of the ratio $|V_{td}/V_{ts}|$, as well as the standard model predictions for the B_s^0-$\overline{B_s^0}$ mixing parameter x_s and the quantities $\sin 2\alpha$, $\sin 2\beta$ and $\sin^2 \gamma$, which characterize the CP-asymmetries in B-decays. The ALEPH collaboration has recently reported a significant improvement on the lower limit on the B_s^0-$\overline{B_s^0}$ mass difference, $\Delta M_s/\Delta M_d > 11.3$ (95% C.L.). This has interesting consequences for the CKM parameters which are also worked out.

---

[*]On leave of absence from DESY, Hamburg, FRG.

1   Introduction

The CDF collaboration at Fermilab has recently published evidence for top quark production in $p\bar{p}$ collisions at $\sqrt{s} = 1.8$ TeV. The search is based on the final states expected in the decays of the top quark in the standard model (SM). Based on this analysis a top quark mass $m_t = 174 \pm 10^{+13}_{-12}$ GeV and a production cross section $\sigma(p\bar{p} \to t\bar{t} + X) = 13.9^{+6.1}_{-4.8}$ pb have been reported [1]. The CDF value for the top quark mass is in very comfortable agreement with the prediction based on the SM fits of the electroweak data from LEP, SLC, CERN and Fermilab colliders and neutrino beams, $m_t = 177 \pm 11^{+18}_{-19}$ GeV [2]. The top quark production cross section measured by CDF is roughly a factor of 2 larger than the expected theoretical value in QCD [1] but is consistent with the upper limit presented by the D0 collaboration: $\sigma(p\bar{p} \to t\bar{t} + X) < 13$ pb (95% C.L.) for a top quark mass of 180 GeV [3]. The neat overlap between the estimates of m_t based on the SM-electroweak analysis and its direct measurement, together with the implied dominance of the decay mode $t \to W^+ b$, is a resounding success of the standard model [4, 5].

It is well appreciated that the top quark plays a crucial role in the phenomenology of the electroweak interactions, flavour mixing, rare decay rates and CP violation [6]. Therefore the new experimental input for m_t, while still not very precise, should help in reducing the present uncertainties on the parameters of the Cabibbo-Kobayashi-Maskawa (CKM) quark mixing matrix [5]. Conversely, the knowledge of m_t can be used to restrict the range of the relevant hadronic matrix elements, which in turn should help in firming up SM-based predictions for rare decays and CP asymmetries in a number of K- and B-hadron decays. This has been the theme of a number of papers which have appeared since the CDF measurement of the top quark mass [7, 8, 9]. In addition, a theoretical analysis along the same lines predated the CDF announcement [10]. In the meantime, a number of parameters crucial for the CKM phenomenology have evolved so that an updated analysis is in order.

The aim of this article is to revise and update the profile of the CKM matrix elements reported earlier by us [7], in particular the CKM unitarity triangle. In doing this update, we also include the improvements reported in a number of measurements of the lifetime, mixing ratio, and the CKM matrix elements $|V_{cb}|$ and $|V_{ub}/V_{cb}|$ from B decays, measured by the ARGUS, CLEO, CDF and LEP experiments. We note here the changes that we have made in the present manuscript compared to our earlier analysis reported in ref. [7]:

- We have scaled the CDF top quark mass $m_t = 174 \pm 16$ GeV to the running top quark mass in the $\overline{MS}$ scheme so as to be able to use consistently the next-to-leading order expressions for the mass differences ΔM_d and ΔM_s and the CP violating parameter $|\epsilon|$ which have been calculated in the $\overline{MS}$ scheme [6, 10]. The correctly scaled value $\overline{m_t}(m_t) = 165 \pm 16$ GeV [11] is about 9 GeV lower than what we had used previously [12]. This renormalization reduces m_t by only $\sim 0.5\sigma$, and hence does not significantly change the results of ref. [7], though its incorporation into the CKM fits does change the central values of the parameters slightly.

- The present knowledge of the CKM matrix element ratio $|V_{ub}/V_{cb}|$ is poor. The only source of information for this ratio so far is the end-point lepton energy spectrum in semileptonic B decays which is model dependent. No new measurement or analysis

of this quantity has been reported since we did our last fits. However, in consultation with our experimental colleagues, we have increased the error on this ratio and now use a value $|V_{ub}/V_{cb}| = 0.08 \pm 0.03$, which better reflects the underlying theoretical dispersion on this ratio.

- New measurements for the quantity $\mathcal{F}(1)|V_{cb}|$ in the decays $B \to D^*\ell\nu_\ell$ using heavy quark effective theory (HQET) methods have been made by the CLEO [13], ARGUS [14] and ALEPH collaborations [15]. In the meantime, estimates for the quantity $\mathcal{F}(1) \equiv \xi(1)\eta_A$ have undergone some revision in both the QCD perturbative part (η_A) and power corrections to the Isgur-Wise function at the symmetry point ($\xi(1)$) [16, 17]. Taking into account the updated experimental and theoretical input, we estimate $|V_{cb}| = 0.039 \pm 0.006$. The central value for this matrix element has moved down by 0.002 compared to the value $|V_{cb}| = 0.041 \pm 0.006$ used by us previously.

- The precision on the B_d^0-$\overline{B_d^0}$ mass difference ΔM_d obtained from time-dependent methods is now better than that on the corresponding time-integrated quantity, $x_d = \Delta M_d/\Gamma_d$. The precision on ΔM_d can be further improved by combining the time-dependent and time-integrated information. The present world average, $\Delta M_d = 0.5 \pm 0.033$ (ps)$^{-1}$ [18], which includes the various systematic uncertainties relevant for the extraction of this quantity, can be directly analysed in terms of the (QCD-corrected) SM estimates of the same. This reduces the error due to the lifetime, which one has to take into account in the analysis of x_d.

- The lower limit on the mass difference ratio $\Delta M_s/\Delta M_d > 11.3$ at 95% C.L., reported by the ALEPH collaboration [19], provides an additional bound on the CKM parameters. Previously, the experimental bound was much lower and hence not very interesting. In our analysis, we present the constraints on the CKM parameters which follow from the ALEPH lower limit on the mass difference ratio.

It should be pointed out that, despite these several changes, the results presented in this paper differ very little from those of ref. [7]. Furthermore, in spite of the benefit of new experimental data, the allowed region for the CKM parameters is still quite large, as we will see. This is because the main uncertainty is theoretical, and is due to our lack of knowledge of hadronic matrix elements. This underlines the crucial importance of measuring CP-violating rate asymmetries in the B system – such asymmetries are independent of hadronic uncertainties, and will thus provide us with *clean* information about the CKM parameters.

In our analysis we consider two types of fits. In Fit 1, we assume particular fixed values for the theoretical hadronic quantities. The allowed ranges for the CKM parameters are derived from the (Gaussian) errors on experimental measurements only. In Fit 2, we assign a central value plus an error (treated as Gaussian) to the theoretical quantities. In the resulting fits, we combine the experimental and theoretical errors in quadrature. For both fits we calculate the allowed region in CKM parameter space at 95% C.L. We also present the corresponding allowed ranges for the CP-violating phases that will be measured in B decays, characterized by $\sin 2\beta$, $\sin 2\alpha$ and $\sin^2 \gamma$. These can be measured directly through rate asymmetries in the decays $\overset{(-)}{B_d} \to J/\psi K_S$, $\overset{(-)}{B_d} \to \pi^+\pi^-$, and $\overset{(-)}{B_s} \to D_s^\pm K^\mp$,

respectively. We also give the allowed domains for two of the angles, $(\sin 2\alpha, \sin 2\beta)$. We estimate the SM prediction for the B_s^0-$\overline{B_s^0}$ mixing parameter, x_s, and show how the ALEPH limit of $x_s > 9.0$ (95% C.L.) constrains the parameter space. Finally, we give the present 95% C.L. upper and lower bounds on the matrix element ratio $|V_{td}/V_{ts}|$.

This paper is organized as follows. In section 2, we present our update of the CKM matrix, concentrating especially on the matrix element $|V_{cb}|$ which, thanks to the progress in HQET and experiments, is now well under control. The constraints that follow from $|V_{ub}/V_{cb}|$, $|\epsilon|$ and ΔM_d on the CKM parameters are also discussed here. Section 3 contains the results of our fits. These results are summarized in terms of the allowed domains of the unitarity triangle, which are displayed in several Figures and Tables. In section 4, we discuss the impact of the recent lower limit on the ratio $\Delta M_s/\Delta M_d$ reported by the ALEPH collaboration on the CKM parameters and estimate the expected range of the mixing ratio x_s in the SM based on our fits. Here we also present the allowed 95% C.L. range for $|V_{td}/V_{ts}|$. In section 5 we discuss the predictions for the CP asymmetries in the neutral B meson sector and calculate the correlations for the CP violating asymmetries proportional to $\sin 2\alpha$, $\sin 2\beta$ and $\sin^2 \gamma$. Section 6 contains a summary and an outlook for improving the profile of the CKM unitarity triangle.

2   An Update of the CKM Matrix

In updating the CKM matrix elements, we make use of the Wolfenstein parametrization [20], which follows from the observation that the elements of this matrix exhibit a hierarchy in terms of λ, the Cabibbo angle. In this parametrization the CKM matrix can be written approximately as

$$V_{CKM} \simeq \begin{pmatrix} 1 - \frac{1}{2}\lambda^2 & \lambda & A\lambda^3 (\rho - i\eta) \\ -\lambda & 1 - \frac{1}{2}\lambda^2 - iA^2\lambda^4\eta & A\lambda^2 \\ A\lambda^3 (1 - \rho - i\eta) & -A\lambda^2 & 1 \end{pmatrix} . \tag{1}$$

In this section we shall discuss those quantities which constrain these CKM parameters, pointing out the significant changes in the determination of λ, A, ρ and η. Recently, the importance of including higher-order terms in the Wolfenstein parametrization given above has been emphasized [10]. This amounts to redefining the parameters ρ and η, with the improved Wolfenstein parameters being $\bar{\rho} = \rho(1 - \lambda^2/2)$ and $\bar{\eta} = \eta(1 - \lambda^2/2)$. While such a procedure may become important when the experimental precision on the CP asymmetries in B decays becomes comparable to $\lambda^2/2 \simeq 3\%$, at present it is unnecessary, and we will continue using the standard Wolfenstein parametrization given above. The error incurred by its use is negligible compared to all the other uncertainties in the CKM fits.

We recall that $|V_{us}|$ has been extracted with good accuracy from $K \to \pi e\nu$ and hyperon decays [21] to be

$$|V_{us}| = \lambda = 0.2205 \pm 0.0018 . \tag{2}$$

This agrees quite well with the determination of $V_{ud} \simeq 1 - \frac{1}{2}\lambda^2$ from β-decay,

$$|V_{ud}| = 0.9744 \pm 0.0010 . \tag{3}$$

3

The parameter A is related to the CKM matrix element V_{cb}, which can be obtained from semileptonic decays of B mesons. We shall restrict ourselves to the methods based on HQET to calculate the exclusive and inclusive semileptonic decay rates. In the heavy quark limit it has been observed that all hadronic form factors in the semileptonic decays $B \to (D, D^*)\ell\nu_\ell$ can be expressed in terms of a single function, the Isgur-Wise function [22]. It has been shown that the HQET-based method works best for $B \to D^* l\nu$ decays, since these are unaffected by $1/m_Q$ corrections [23, 24, 25]. This method has been used by the ALEPH, ARGUS and CLEO collaborations to determine $\xi(1)|V_{cb}|$ and the slope of the Isgur-Wise function.

Using HQET, the differential decay rate in $B \to D^*\ell\nu_\ell$ is

$$
\frac{d\Gamma(B \to D^*\ell\bar{\nu})}{d\omega} = \frac{G_F^2}{48\pi^3}(m_B - m_{D^*})^2 m_{D^*}^3 \eta_A^2 \sqrt{\omega^2 - 1}(\omega + 1)^2 \tag{4}
$$
$$
\times [1 + \frac{4\omega}{\omega + 1}\frac{1 - 2\omega r + r^2}{(1 - r)^2}]|V_{cb}|^2\xi^2(\omega) ,
$$

where $r = m_{D^*}/m_B$, $\omega = v \cdot v'$ (v and v' are the four-velocities of the B and D^* meson, respectively), and η_A is the short-distance correction to the axial vector form factor. In the leading logarithmic approximation, this was calculated by Shifman and Voloshin some time ago – the so-called hybrid anomalous dimension [26]. In the absence of any power corrections, $\xi(\omega = 1) = 1$. The size of the $O(1/m_b^2)$ and $O(1/m_c^2)$ corrections to the Isgur-Wise function $\xi(\omega)$, and to some extent the next-to-leading order corrections to η_A have recently become a matter of some discussion [16, 17, 27]. We recall that the effects of such power corrections were previously estimated as [27]

$$
\xi(1) = 1 + \delta(1/m^2) = 0.98 \pm 0.04 ,
$$
$$
\eta_A = 0.99 , \tag{5}
$$

and the corresponding corrections to $\xi(1)$ were estimated by Mannel [28] to be

$$
-0.05 < \xi(1) - 1 < 0 . \tag{6}
$$

In a recent paper Shifman, Uraltsev and Vainshtain [17] have argued that the deviation of $\xi(1)$, as well as that of η_A, from unity is larger than the estimate given in eq. (5). Following ref. [17], this deviation can be expressed as

$$
1 - \xi^2(1) = \frac{1}{3}\frac{\mu_G^2}{m_c^2} + \frac{\mu_\pi^2 - \mu_G^2}{4}(\frac{1}{m_c^2} + \frac{1}{m_b^2} + \frac{2}{3m_c m_b}) + \sum_{i=1,2,...} \xi_{B \to excit}^2 , \tag{7}
$$

where the contribution to the higher excited states is indicated by the last term, and μ_G^2 and μ_π^2 parametrize the matrix elements of the chromomagnetic and kinetic energy operators, respectively. These have been estimated to be

$$
\mu_G^2 = \frac{3}{4}(M_{B^*}^2 - M_B^2) \simeq 0.35 \text{ GeV}^2, \tag{8}
$$
$$
\mu_\pi^2 = (0.54 \pm 0.12) \text{ GeV}^2 ,
$$

where the numbers for μ_π^2 are based on QCD sum rules [29]. Using the central value for this quantity and ignoring the contribution of the excited states, one gets (henceforth we use $\mathcal{F}(1) \equiv \eta_A \xi(1)$)

$$\mathcal{F}(1) = 0.92 \ . \tag{9}$$

The contribution of the higher states is positive definite. However, its actual value can only be guessed at present. Shifman et al. estimate [17]

$$\mathcal{F}(1) = 0.89 \pm 0.03 \ . \tag{10}$$

In the meantime, Neubert has revised his estimate of the same quantity (we refer to ref. [16] for details), obtaining

$$\mathcal{F}(1) = 0.93 \pm 0.03 \ . \tag{11}$$

The values of $\mathcal{F}(1)$ given in eqs. (10) and (11) are significantly smaller than unity and one must conclude that the $O(1/m_Q^2)$ corrections to $\xi(1)$ are important numerically. However, the theoretical estimates by Neubert and Shifman et al. are now compatible with each other, within quoted errors. In the analysis for $|V_{cb}|$ presented here, we shall use the range

$$\mathcal{F}(1) = 0.91 \pm 0.05 \ , \tag{12}$$

which covers the ($\pm 1\sigma$) range in the two estimates, giving an intrinsic theoretical error $\Delta|V_{cb}|/|V_{cb}| = 0.06$ from corrections to $\mathcal{F}(1)$. To further reduce this error a better estimate for the excited states is needed. This might be forthcoming when the contribution of the inelastic channels in semileptonic B decays is measured more accurately.

As already mentioned in the introduction, the experimental measurements have also evolved in time. The previously reported value for $|V_{cb}|$ by the ARGUS collaboration from the decays $B \rightarrow D^* + \ell\bar{\nu}$ using the HQET formalism yielded a value $|V_{cb}| = 0.047 \pm 0.007$ with a considerably higher value for the slope of the Isgur-Wise function, $\xi'(1) \equiv -\rho^2$, in the range $1.9 < \rho^2 < 2.3$ [30]. In a recent analysis by ARGUS, significantly lower values for both $|V_{cb}|$ and ρ^2 have been obtained, yielding [14]

$$\mathcal{F}(1)|V_{cb}|(\frac{\tau(B_d^0)}{1.53 \text{ ps}})^{1/2} = 0.039 \pm 0.004 \pm 0.003 \ ,$$
$$\rho^2 = 1.08 \pm 0.12 \ , \tag{13}$$

where the value of $|V_{cb}|$ corresponds to a linear extrapolation of the Isgur-Wise function $\xi(\omega) = 1 - \rho^2(\omega - 1)$, and the error quoted includes that from the B_d^0 lifetime.

The numbers obtained by the CLEO collaboration using a similar method are [13]

$$\mathcal{F}(1)|V_{cb}|(\frac{\tau(B_d^0)}{1.53 \text{ ps}})^{1/2} = 0.0351 \pm 0.0019 \pm 0.0022 \ ,$$
$$\rho^2 = 0.84 \pm 0.12 \pm 0.08 \ , \tag{14}$$

where the numbers correspond to a linear extrapolation of the Isgur-Wise function. The error quoted includes also that from the B lifetime, $\tau(B_d^0) = 1.53 \pm 0.09$ (ps). The slope of the Isgur-Wise function has also been measured by the CLEO collaboration through

an independent method which yields in addition the ratios of the vector and axial vector form factors in the decay $B \to D^* \ell / \nu_\ell$. The resulting slope [31],

$$\rho^2 = 1.01 \pm 0.15 \pm 0.09 , \tag{15}$$

is consistent with that given in eq. (14), though the central value is larger. The third measurement along the same lines has been undertaken by the ALEPH collaboration. Their analysis yields

$$\mathcal{F}(1)|V_{cb}|(\frac{\tau(B_d^0)}{1.53 \text{ ps}})^{1/2} = 0.0392 \pm 0.0044 \pm 0.0035 ,$$
$$\rho^2 = 0.46 \pm 0.30 \pm 0.15 . \tag{16}$$

All three measurements of the quantity $\mathcal{F}(1)|V_{cb}|$ are compatible with one another. The slope parameter in eqs. (13) and (15) are very close to each other, with the ALEPH value lower but consistent with the other two. All three measurements are in agreement with the theoretical bounds, which suggest $\rho^2 \leq 1$ [32, 33].

The ALEPH, ARGUS and CLEO values of $\mathcal{F}(1)|V_{cb}|$ given above have been averaged by taking into account various common and independent systematic errors, yielding [34]

$$\mathcal{F}(1)|V_{cb}| = 0.036 \pm 0.003 . \tag{17}$$

Taking into account the theoretical estimate of the renormalized Isgur-Wise function $\mathcal{F}(1) = 0.91 \pm 0.05$, the updated value for $|V_{cb}|$ can be expressed as

$$|V_{cb}| = 0.0395 \pm 0.003 \pm 0.001 \pm 0.002 , \tag{18}$$

where, following the advice in refs. [34, 35], an overall systematic error of ± 0.001 has been added to take into account the slope of the Isgur-Wise function; ± 0.002 represents the theoretical error due to $\mathcal{F}(1)$. Using the same data but taking instead the estimate for $\mathcal{F}(1)$ in eq. (11), Neubert has obtained the following number for $|V_{cb}|$ [16]:

$$|V_{cb}| = 0.0399 \pm 0.0026(\text{exp}) \pm 0.0013(\text{th}) , \tag{19}$$

getting $|V_{cb}| = 0.0399 \pm 0.0029$, adding all errors in quadrature. The central values for $|V_{cb}|$ in (18) and (19) are practically identical, but the associated errors are different. In our opinion, it is perhaps prudent to add the errors linearly to have a reliable determination of $|V_{cb}|$. For the purposes of the fits which follow, we shall use the following value of $|V_{cb}|$:

$$|V_{cb}| = 0.039 \pm 0.006 , \tag{20}$$

which yields for the CKM parameter A,

$$A = 0.80 \pm 0.12 . \tag{21}$$

The above value for $|V_{cb}|$ is in broad agreement with the values obtained using other theoretical techniques for the exclusive and inclusive semileptonic decays. We mention

here the lattice-QCD based calculation of the Isgur-Wise function by the UKQCD collaboration which, when combined with the CLEO and ARGUS data, yields [36]

$$|V_{cb}| = 0.037 \pm 0.001 \pm 0.002^{+0.008}_{-0.003} , \qquad (22)$$

where we have updated the published UKQCD number for the current value of the B lifetime. The updated number [37] from the lattice-based calculation in ref. [38] is

$$|V_{cb}| = 0.044 \pm 0.007 \pm 0.005 . \qquad (23)$$

Likewise, a calculation using the QCD sum rules yields [39]

$$|V_{cb}| = 0.0382 \pm 0.0012 \pm 0.0015 \pm 0.0015 , \qquad (24)$$

where the first error is experimental and the other two are related to theoretical effects. Inclusive semileptonic decay rates have also been calculated using HQET methods [17, 40, 41] which require the knowledge of the quark mass difference $(m_b - m_c)$, the B semileptonic branching ratio, and the B lifetime. There exists at present some dispersion in the theoretical estimates of the quark masses and the mass difference, which leads to significantly different determinations of the matrix element $|V_{cb}|$. The determination of $|V_{cb}|$ using this method and data from $\Upsilon(4S)$ and Z decays is summarized in ref. [35]:

$$
\begin{aligned}
\Upsilon(4S): & \quad |V_{cb}| &=& \quad 0.039 \pm 0.001 \pm 0.005 & \quad (\tau(B) = 1.63 \pm 0.07 \text{ ps}), \\
Z: & \quad |V_{cb}| &=& \quad 0.042 \pm 0.002 \pm 0.005 & \quad (\tau(b) = 1.55 \pm 0.06 \text{ ps}),
\end{aligned} \qquad (25)
$$

where the second error reflects theoretical dispersion. One notices a remarkable consistency in $|V_{cb}|$ from the $\Upsilon(4S)$ data using the inclusive semileptonic rate and the corresponding number determined from the exclusive decay $B \to D^* \ell \nu_\ell$ in the HQET approach, though the present theoretical errors in the former are somewhat larger.

The other two CKM parameters ρ and η are constrained by the measurements of $|V_{ub}/V_{cb}|$, $|\epsilon|$ (the CP-violating parameter in the kaon system), x_d (B_d^0-$\overline{B_d^0}$ mixing) and (in principle) ϵ'/ϵ ($\Delta S = 1$ CP-violation in the kaon system). We shall not discuss the constraints from ϵ'/ϵ, due to the various experimental and theoretical uncertainties surrounding it at present, but take up the rest in turn and present fits in which the allowed region of ρ and η is shown.

First of all, $|V_{ub}/V_{cb}|$ can be obtained by looking at the endpoint of the inclusive lepton spectrum in semileptonic B decays. Unfortunately, there still exists quite a bit of model dependence in the interpretation of data. The present average of this ratio, based on the recent analysis of the ARGUS [42] and CLEO [43, 44] data, is [34]

$$\left| \frac{V_{ub}}{V_{cb}} \right| = 0.08 \pm 0.03 . \qquad (26)$$

This gives

$$\sqrt{\rho^2 + \eta^2} = 0.36 \pm 0.14 . \qquad (27)$$

This is significantly less precise than the corresponding range used by us [7] and others [8, 9, 10], and has important consequences for the CKM fits.

The experimental value of $|\epsilon|$ is [21]

$$|\epsilon| = (2.26 \pm 0.02) \times 10^{-3} . \tag{28}$$

Theoretically, $|\epsilon|$ is essentially proportional to the imaginary part of the box diagram for K^0-$\overline{K^0}$ mixing and is given by [45]

$$\begin{aligned}
|\epsilon| &= \frac{G_F^2 f_K^2 M_K M_W^2}{6\sqrt{2}\pi^2 \Delta M_K} \hat{B}_K \left(A^2\lambda^6\eta\right) \left(y_c \left\{\hat{\eta}_{ct} f_3(y_c, y_t) - \hat{\eta}_{cc}\right\}\right. \\
&\quad + \left. \hat{\eta}_{tt} y_t f_2(y_t) A^2\lambda^4(1-\rho)\right).
\end{aligned} \tag{29}$$

Here, the $\hat{\eta}_i$ are QCD correction factors, of which $\hat{\eta}_{cc}$ and $\hat{\eta}_{tt}$ have been calculated to next-to-leading order, and, to the best of our knowledge, $\hat{\eta}_{ct}$ has so far been calculated to leading order. The renormalization-scale invariant coefficients have the value $\hat{\eta}_{cc} \simeq 1.10$ [46], $\hat{\eta}_{tt} \simeq 0.57$ [47], $\hat{\eta}_{ct} \simeq 0.36$ for $\Lambda_{QCD} = 200$ MeV [6, 48]. In eq. (29), $y_i \equiv m_i^2/M_W^2$, and the functions f_2 and f_3 are given by

$$\begin{aligned}
f_2(x) &= \frac{1}{4} + \frac{9}{4}\frac{1}{(1-x)} - \frac{3}{2}\frac{1}{(1-x)^2} - \frac{3}{2}\frac{x^2\ln x}{(1-x)^3} , \\
f_3(x, y) &= \ln\frac{y}{x} - \frac{3y}{4(1-y)}\left(1 + \frac{y}{1-y}\ln y\right).
\end{aligned} \tag{30}$$

(The above form for $f_3(x, y)$ is an approximation, obtained in the limit $x \ll y$. For the exact expression, see ref. [49].)

The final parameter in the expression for $|\epsilon|$ is the renormalization-scale independent parameter $\hat{B}_K$, which represents our ignorance of the hadronic matrix element $\langle K^0|(\overline{d}\gamma^\mu(1-\gamma_5)s)^2|\overline{K^0}\rangle$. The evaluation of this matrix element has been the subject of much work. The earlier results are summarized in ref. [50]. For a recent comparative study of the various calculational techniques, in particular a critical review of the chiral perturbation theory based estimates, see ref. [8], which advocates a range $\hat{B}_K = 0.50 \pm 0.15$, termed as "best estimates," and $\hat{B}_K = 0.55 \pm 0.25$ as the so-called "conservative choice," rendering this quantity uncertain to more than a factor of 2. We note here that significant progress in lattice-QCD methods has been made in determining $\hat{B}_K$ [51], based on a better understanding of the perturbative corrections to lattice operators, finite lattice-size effects, and first estimates of effects due to dynamical quarks. The present lattice QCD estimate gives (Gupta et al. in ref. [52])

$$\hat{B}_K = 0.82 \pm 0.027 \pm 0.023 . \tag{31}$$

In our first set of fits, we consider specific values in the range 0.4 to 1.0 for $\hat{B}_K$. As we shall see, for $\hat{B}_K = 0.4$ a poor fit to the data is obtained, so that such small values are somewhat disfavoured. In Fit 2, we assign a central value plus an error to $\hat{B}_K$. In order to reflect the estimates of this quantity in lattice QCD [52], we take

$$\hat{B}_K = 0.8 \pm 0.2 . \tag{32}$$

In order to see the sensitivity of the allowed range of the CKM parameters to a lower value of $\hat{B}_K$, we also present fits for the range

$$\hat{B}_K = 0.6 \pm 0.2 , \tag{33}$$

Parameter	Value
λ	0.2205
$|V_{cb}|$	0.039 ± 0.006
$|V_{ub}/V_{cb}|$	0.08 ± 0.03
$|\epsilon|$	$(2.26 \pm 0.02) \times 10^{-3}$
ΔM_d	$(0.50 \pm 0.033) \ (\mathrm{ps})^{-1}$
$\overline{m_t}(m_t(pole))$	$(165 \pm 16) \ \mathrm{GeV}$
$\hat{\eta}_B$	0.55
$\hat{\eta}_{cc}$	1.10
$\hat{\eta}_{ct}$	0.36
$\hat{\eta}_{tt}$	0.57
$\hat{B}_K$	0.8 ± 0.2
$\hat{B}_B$	1.0 ± 0.2
f_{B_d}	$180 \pm 50 \ \mathrm{MeV}$

Table 1: Parameters used in the CKM fits. Values of the hadronic quantities f_{B_d}, $\hat{B}_{B_d}$ and $\hat{B}_K$ shown are motivated by the lattice QCD results. In Fit 1, specific values of these hadronic quantities are chosen, while in Fit 2, they are allowed to vary over the given ranges. (In Fit 2, for comparison we also consider the range $\hat{B}_K = 0.6 \pm 0.2$, which is motivated by chiral perturbation theory and QCD sum rules.)

which overlaps with the values suggested by chiral perturbation theory. As we will see, there is not an enormous difference in the results for the two ranges.

We now turn to B_d^0-$\overline{B_d^0}$ mixing. The present world average of $x_d \equiv \Delta M_d/\Gamma_d$, which is a measure of this mixing, is [18]

$$x_d = 0.76 \pm 0.06 \ , \tag{34}$$

which is based on time-integrated measurements which directly measure x_d, and on time-dependent measurements which measure the mass difference ΔM_d directly. This is then converted to x_d using the B_d^0 lifetime. From a theoretical point of view it is better to use the mass difference ΔM_d, as it liberates one from the errors on the lifetime measurement. In fact, the present precision on ΔM_d, pioneered by time-dependent techniques at LEP, is quite competitive with the precision on x_d. The LEP-average $\Delta M_d = 0.513 \pm 0.036$ $(\mathrm{ps})^{-1}$ has been combined with that derived from time-integrated measurements yielding the present world average [18]

$$\Delta M_d = 0.500 \pm 0.033 \ (\mathrm{ps})^{-1} \ . \tag{35}$$

We shall use this number instead of x_d, which has been the usual practice to date [6]-[10].

The mass difference ΔM_d is calculated from the B_d^0-$\overline{B_d^0}$ box diagram. Unlike the kaon system, where the contributions of both the c- and the t-quarks in the loop were important, this diagram is dominated by t-quark exchange:

$$\Delta M_d = \frac{G_F^2}{6\pi^2} M_W^2 M_B \left(f_{B_d}^2 \hat{B}_{B_d} \right) \hat{\eta}_B y_t f_2(y_t) |V_{td}^* V_{tb}|^2 \ , \tag{36}$$

where, using eq. 1, $|V_{td}^* V_{tb}|^2 = A^2\lambda^6 \left[(1-\rho)^2 + \eta^2\right]$. Here, $\hat{\eta}_B$ is the QCD correction. In ref. [47], this correction is analyzed including the effects of a heavy t-quark. It is found that $\hat{\eta}_B$ depends sensitively on the definition of the t-quark mass, and that, strictly speaking, only the product $\hat{\eta}_B(y_t)f_2(y_t)$ is free of this dependence. In the fits presented here we use the value $\hat{\eta}_B = 0.55$, calculated in the $\overline{MS}$ scheme, following ref. [47]. Consistency requires that the top quark mass be rescaled from its pole (mass) value of $m_t = 174 \pm 16$ GeV to the value $\overline{m_t}(m_t(pole))$ in the $\overline{MS}$ scheme, which is typically about 9 GeV smaller [11, 12].

For the B system, the hadronic uncertainty is given by $f_{B_d}^2 \hat{B}_{B_d}$, analogous to $\hat{B}_K$ in the kaon system, except that in this case, also f_{B_d} is not measured. The lattice-QCD results for these hadronic quantities have been recently summarized as follows [51]:

$$
\begin{aligned}
f_{B_d} &= 180 \pm 40 \text{ MeV}, \\
\hat{B}(B_d) &= 1.2 \pm 0.2,
\end{aligned}
\tag{37}
$$

while the corresponding numbers from the QCD sum rules are [53]

$$
\begin{aligned}
f_{B_d} &= (1.60 \pm 0.26)f_\pi, \\
\hat{B}(B_d) &= 1.0 \pm 0.15.
\end{aligned}
\tag{38}
$$

In our fits, we will take ranges for $f_{B_d}^2 \hat{B}_{B_d}$ and $\hat{B}_{B_d}$ which are compatible with both of the above sets of numbers [51, 53, 54]:

$$
\begin{aligned}
f_{B_d} &= 180 \pm 50 \text{ MeV}, \\
\hat{B}_{B_d} &= 1.0 \pm 0.2.
\end{aligned}
\tag{39}
$$

In Table 1, we summarize all input quantities to our fits.

3 The Unitarity Triangle

The allowed region in ρ-η space can be displayed quite elegantly using the so-called unitarity triangle. The unitarity of the CKM matrix leads to the following relation:

$$
V_{ud}V_{ub}^* + V_{cd}V_{cb}^* + V_{td}V_{tb}^* = 0 .
\tag{40}
$$

Using the form of the CKM matrix in eq. 1, this can be recast as

$$
\frac{V_{ub}^*}{\lambda V_{cb}} + \frac{V_{td}}{\lambda V_{cb}} = 1 ,
\tag{41}
$$

which is a triangle relation in the complex plane (i.e. ρ-η space), illustrated in Fig. 1. Thus, allowed values of ρ and η translate into allowed shapes of the unitarity triangle.

In order to find the allowed unitarity triangles, the computer program MINUIT is used to fit the CKM parameters A, ρ and η to the experimental values of $|V_{cb}|$, $|V_{ub}/V_{cb}|$, $|\epsilon|$ and x_d. Since λ is very well measured, we have fixed it to its central value given above. As discussed in the introduction, we present here two types of fits:
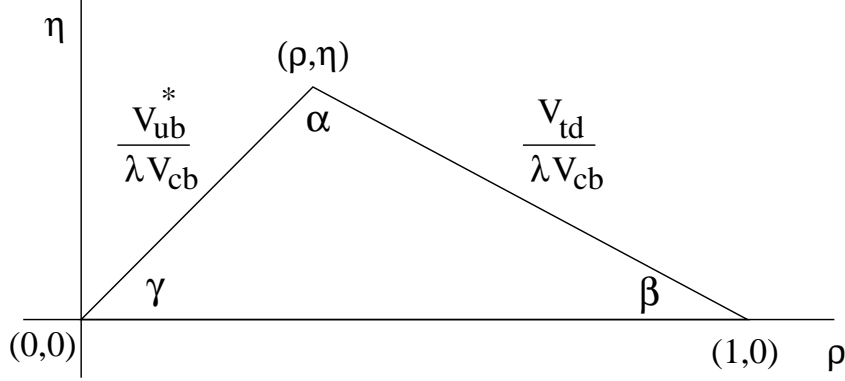
Figure 1: The unitarity triangle. The angles α, β and γ can be measured via CP violation in the B system.

- Fit 1: the "experimental fit." Here, only the experimentally measured numbers are used as inputs to the fit with Gaussian errors; the coupling constants $f_{B_d}\sqrt{\hat{B}_{B_d}}$ and $\hat{B}_K$ are given fixed values.

- Fit 2: the "combined fit." Here, both the experimental and theoretical numbers are used as inputs assuming Gaussian errors for the theoretical quantities.

We first discuss the "experimental fit" (Fit 1). The goal here is to restrict the allowed range of the parameters (ρ, η) for given values of the coupling constants $f_{B_d}\sqrt{\hat{B}_{B_d}}$ and $\hat{B}_K$. For each value of $\hat{B}_K$ and $f_{B_d}\sqrt{\hat{B}_{B_d}}$, the CKM parameters A, ρ and η are fit to the experimental numbers given in Table 1 and the χ^2 is calculated.

First, we fix $\hat{B}_K = 0.8$, and vary $f_{B_d}\sqrt{\hat{B}_{B_d}}$ in the range 130 MeV to 230 MeV. The fits are presented as an allowed region in ρ-η space at 95% C.L. ($\chi^2 = \chi^2_{min} + 6.0$). The results are shown in Fig. 2. As we pass from Fig. 2(a) to Fig. 2(e), the unitarity triangles represented by these graphs become more and more obtuse. Even more striking than this, however, is the fact that the range of possibilities for these triangles is enormous. There are two things to be learned from this. First, our knowledge of the unitarity triangle is at present rather poor. This will be seen even more clearly when we present the results of Fit 2. Second, unless our knowledge of hadronic matrix elements improves considerably, measurements of $|\epsilon|$ and x_d, no matter how precise, will not help much in further constraining the unitarity triangle. This is why measurements of CP-violating rate asymmetries in the B system are so important [55, 56]. Being largely independent of theoretical uncertainties, they will allow us to accurately pin down the unitarity triangle. With this knowledge, we could deduce the correct values of $\hat{B}_K$ and $f_{B_d}\sqrt{\hat{B}_{B_d}}$, and thus rule out or confirm different theoretical approaches to calculating these hadronic quantities.

Despite the large allowed region in the ρ-η plane, certain values of $\hat{B}_K$ and $f_{B_d}\sqrt{\hat{B}_{B_d}}$ are disfavoured since they do not provide a good fit to the data. For example, fixing $\hat{B}_K = 1.0$, we can use the fitting program to provide the minimum χ^2 for various values of $f_{B_d}\sqrt{\hat{B}_{B_d}}$. The results are shown in Table 2, along with the best fit values of (ρ, η). Since we have two variables (ρ and η), we use $\chi^2_{min} < 2.0$ as our "good fit" criterion, and
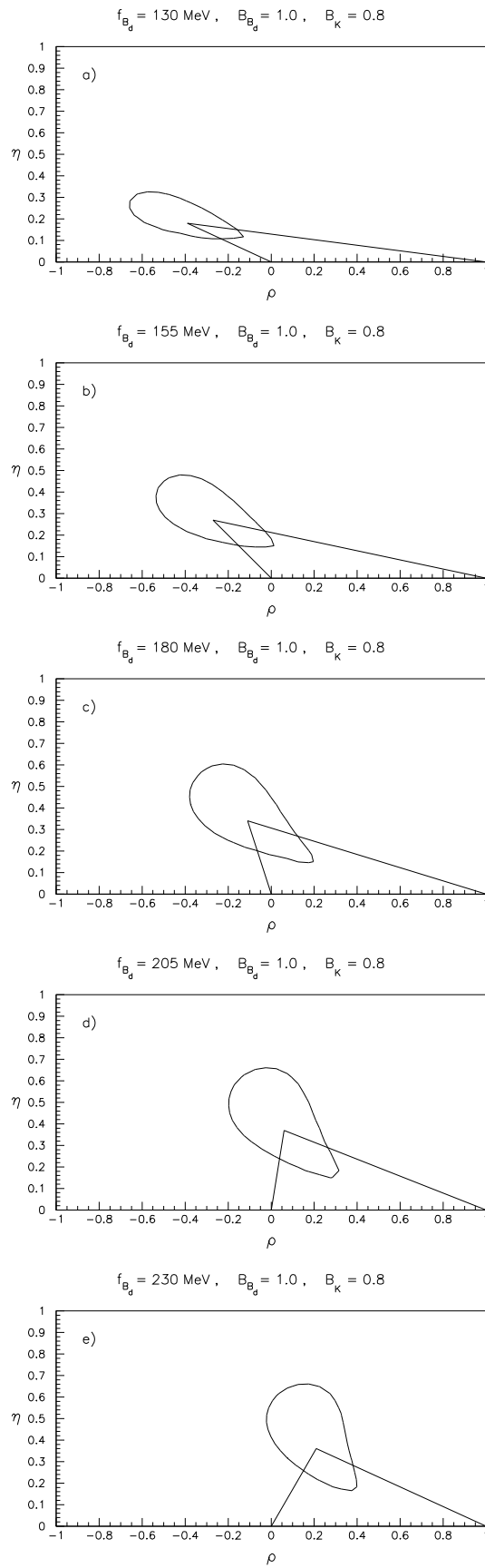
11

Figure 2: Allowed region in ρ-η space, from a fit to the experimental values given in Table 1. We have fixed $\hat{B}_K = 0.8$ and vary the coupling constant product $f_{B_d}\sqrt{\hat{B}_{B_d}}$ as indicated on the figures. The solid line represents the region with $\chi^2 = \chi^2_{min} + 6$ corresponding to the 95% C.L. region. The triangles show the best fit.
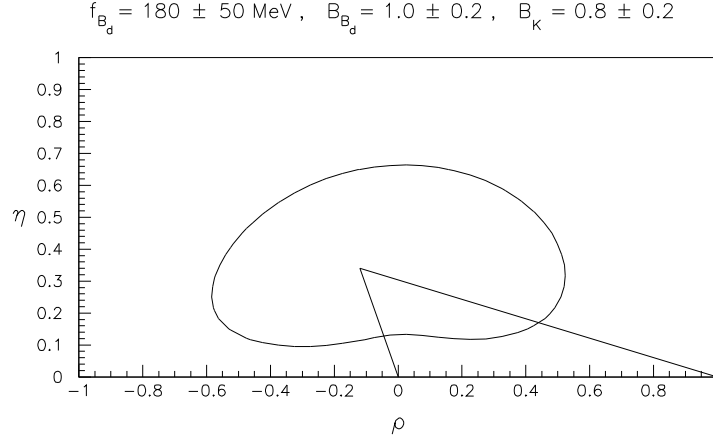
$f_{B_d} = 180 \pm 50$ MeV , $B_{B_d} = 1.0 \pm 0.2$, $B_K = 0.8 \pm 0.2$

Figure 3: Allowed region in ρ-η space, from a simultaneous fit to both the experimental and theoretical quantities given in Table 1. The theoretical errors are treated as Gaussian for this fit. The solid line represents the region with $\chi^2 = \chi^2_{min} + 6$ corresponding to the 95% C.L. region. The triangle shows the best fit.

we see that $f_{B_d}\sqrt{\hat{B}_{B_d}} < 120$ MeV and $f_{B_d}\sqrt{\hat{B}_{B_d}} > 290$ MeV give poor fits to the existing data. Note also that the χ^2 distribution has two minima, at around $f_{B_d}\sqrt{\hat{B}_{B_d}} = 160$ and 230 MeV. We do not consider this terribly significant, since the surrounding values of $f_{B_d}\sqrt{\hat{B}_{B_d}}$ also yield good fits to the data. The very small values of χ^2_{min} depend sensitively on the central values of the various experimental quantities – if these values move around a little bit, the values of $f_{B_d}\sqrt{\hat{B}_{B_d}}$ which give the minimum χ^2 values will move around as well. In Tables 3, 4 and 5, we present similar analyses, but for $\hat{B}_K = 0.8$, 0.6 and 0.4, respectively. From these tables we see that the lower limit on $f_{B_d}\sqrt{\hat{B}_{B_d}}$ remains fairly constant, at around 120 MeV, but the upper limit depends quite strongly on the value of $\hat{B}_K$ chosen. Specifically, for $\hat{B}_K = 0.8$, 0.6 and 0.4, the maximum allowed value of $f_{B_d}\sqrt{\hat{B}_{B_d}}$ is about 270, 230 and 180 MeV, respectively. Note that, for the lower value $\hat{B}_K = 0.4$, which is not favoured by lattice calculations or QCD sum rules, the allowed range of $f_{B_d}\sqrt{\hat{B}_{B_d}}$ is quite restricted, with generally higher values of χ^2 than for the cases of $\hat{B}_K$ in the range 0.6-1.0. This suggests that the data disfavour (though do not completely exclude) $\hat{B}_K \leq 0.4$ solutions. Summing up, present data exclude all values of $f_{B_d}\sqrt{f_{B_d}}$ which lie below 110 MeV and above 290 MeV for the entire $\hat{B}_K$ range.

We now discuss the "combined fit" (Fit 2). Strictly speaking, this fit is not on the same footing as the "experimental fit" presented above, since theoretical "errors" are not Gaussian. On the other hand, experimental systematic errors are also not Gaussian, but it is common practice to treat them as such, and to add them in quadrature with statistical errors. It is in this spirit that we use this method. Since the coupling constants are not known and the best we have are estimates given in the ranges in eqs. (32) and (39), a reasonable profile of the unitarity triangle at present can be obtained by letting the coupling constants vary in these ranges. The resulting CKM triangle region is shown in Fig. 3. As is clear from this figure, the allowed region is enormous! We really know rather little about the unitarity triangle. Even so, its allowed region is still reduced compared to the previous such analyses, due to the knowledge of m_t. The preferred values obtained from the "combined fit" are

$$(\rho, \eta) = (-0.12, 0.34) \quad (\text{with } \chi^2 = 1.1 \times 10^{-3}) . \tag{42}$$

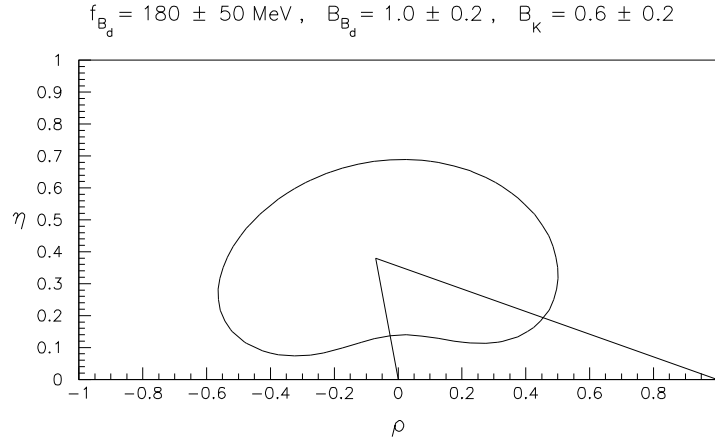For comparison, we also show the allowed region in the (ρ, η) plane for the case in

13

Figure 4: Allowed region in ρ-η space, from a simultaneous fit to both the experimental and theoretical quantities given in Table 1, except that we take $\hat{B}_K = 0.6 \pm 0.2$. The theoretical errors are treated as Gaussian for this fit. The solid line represents the region with $\chi^2 = \chi^2_{min} + 6$ corresponding to the 95% C.L. region. The triangle shows the best fit.

$f_{B_d}\sqrt{\hat{B}_{B_d}}$ (MeV)	(ρ, η)	χ^2_{min}
110	$(-0.48,\ 0.10)$	3.24
120	$(-0.44,\ 0.12)$	1.77
130	$(-0.40,\ 0.15)$	0.85
140	$(-0.36,\ 0.18)$	0.33
150	$(-0.32,\ 0.21)$	7.6×10^{-2}
160	$(-0.28,\ 0.24)$	1.1×10^{-3}
170	$(-0.23,\ 0.27)$	2.4×10^{-2}
180	$(-0.17,\ 0.29)$	8.0×10^{-2}
190	$(-0.11,\ 0.32)$	0.12
200	$(-0.04,\ 0.33)$	0.13
210	$(0.03,\ 0.33)$	8.5×10^{-2}
220	$(0.09,\ 0.33)$	2.8×10^{-2}
230	$(0.15,\ 0.33)$	4.5×10^{-5}
240	$(0.21,\ 0.33)$	4.4×10^{-2}
250	$(0.25,\ 0.33)$	0.18
260	$(0.29,\ 0.33)$	0.43
270	$(0.33,\ 0.33)$	0.77
280	$(0.37,\ 0.33)$	1.21
290	$(0.40,\ 0.33)$	1.73
300	$(0.43,\ 0.32)$	2.34

Table 2: The "best values" of the CKM parameters (ρ, η) as a function of the coupling constant $f_{B_d}\sqrt{\hat{B}_{B_d}}$, obtained by a minimum χ^2 fit to the experimental data, including the renormalized value of $m_t = 165 \pm 16$ GeV. We fix $\hat{B}_K = 1.0$. The resulting minimum χ^2 values from the MINUIT fits are also given.

$f_{B_d}\sqrt{\hat{B}_{B_d}}$ (MeV)	(ρ, η)	χ^2_{min}
110	$(-0.47,\ 0.12)$	3.29
120	$(-0.43,\ 0.15)$	1.83
130	$(-0.39,\ 0.18)$	0.92
140	$(-0.34,\ 0.22)$	0.40
150	$(-0.30,\ 0.25)$	0.13
160	$(-0.24,\ 0.29)$	2.7×10^{-2}
170	$(-0.18,\ 0.32)$	8.6×10^{-4}
180	$(-0.11,\ 0.34)$	1.3×10^{-3}
190	$(-0.04,\ 0.36)$	9.2×10^{-4}
200	$(0.03,\ 0.36)$	1.9×10^{-3}
210	$(0.10,\ 0.37)$	3.1×10^{-2}
220	$(0.16,\ 0.37)$	0.13
230	$(0.21,\ 0.36)$	0.32
240	$(0.26,\ 0.36)$	0.64
250	$(0.31,\ 0.36)$	1.07
260	$(0.35,\ 0.36)$	1.62
270	$(0.39,\ 0.36)$	2.28

Table 3: The "best values" of the CKM parameters (ρ, η) as a function of the coupling constant $f_{B_d}\sqrt{\hat{B}_{B_d}}$, obtained by a minimum χ^2 fit to the experimental data, including the renormalized value of $m_t = 165 \pm 16$ GeV. We fix $\hat{B}_K = 0.8$. The resulting minimum χ^2 values from the MINUIT fits are also given.

$f_{B_d}\sqrt{\hat{B}_{B_d}}$ (MeV)	(ρ, η)	χ^2_{min}
110	$(-0.47,\ 0.16)$	3.40
120	$(-0.42,\ 0.20)$	1.98
130	$(-0.36,\ 0.24)$	1.09
140	$(-0.31,\ 0.28)$	0.58
150	$(-0.25,\ 0.32)$	0.31
160	$(-0.18,\ 0.35)$	0.18
170	$(-0.10,\ 0.38)$	0.15
180	$(-0.03,\ 0.40)$	0.18
190	$(0.05,\ 0.40)$	0.29
200	$(0.12,\ 0.41)$	0.50
210	$(0.19,\ 0.41)$	0.87
220	$(0.24,\ 0.40)$	1.33
230	$(0.30,\ 0.40)$	1.98
240	$(0.35,\ 0.40)$	2.79

Table 4: The "best values" of the CKM parameters (ρ, η) as a function of the coupling constant $f_{B_d}\sqrt{\hat{B}_{B_d}}$, obtained by a minimum χ^2 fit to the experimental data, including the renormalized value of $m_t = 165 \pm 16$ GeV. We fix $\hat{B}_K = 0.6$. The resulting minimum χ^2 values from the MINUIT fits are also given.

$f_{B_d}\sqrt{\hat{B}_{B_d}}$ (MeV)	(ρ, η)	χ^2_{min}
120	$(-0.38,\ 0.29)$	2.41
130	$(-0.31,\ 0.34)$	1.62
140	$(-0.23,\ 0.38)$	1.20
150	$(-0.14,\ 0.42)$	1.06
160	$(-0.05,\ 0.44)$	1.13
170	$(0.04,\ 0.45)$	1.41
180	$(0.12,\ 0.46)$	1.91
190	$(0.19,\ 0.46)$	2.65

Table 5: The "best values" of the CKM parameters (ρ, η) as a function of the coupling constant $f_{B_d}\sqrt{\hat{B}_{B_d}}$, obtained by a minimum χ^2 fit to the experimental data, including the renormalized value of $m_t = 165 \pm 16$ GeV. We fix $\hat{B}_K = 0.4$. The resulting minimum χ^2 values from the MINUIT fits are also given.

which $\hat{B}_K = 0.6 \pm 0.2$ [eq. (33)], which is more favoured by chiral perturbation theory and QCD sum rules. The CKM triangle region is shown in Fig. 4. Clearly, there is not much difference between this figure and Fig. 3. The preferred values obtained from this fit are

$$(\rho, \eta) = (-0.07, 0.38) \quad (\text{with } \chi^2 = 0.13) . \tag{43}$$

We note that the preferred values for (ρ, η) yield the following preferred values for the matrix element ratio $|V_{td}/V_{ts}|$:

$$\frac{|V_{td}|}{|V_{ts}|} = 0.26 \quad [\text{for } \hat{B}_K = 0.6 \pm 0.2] ,$$

$$\frac{|V_{td}|}{|V_{ts}|} = 0.25 \quad [\text{for } \hat{B}_K = 0.8 \pm 0.2] . \tag{44}$$

Such values would make a number of measurements in CKM-suppressed rare decays such as $B \to (\rho, \omega) + \gamma$ much more accessible experimentally.

4 x_s and the Unitarity Triangle

Mixing in the B_s^0-$\overline{B_s^0}$ system is quite similar to that in the B_d^0-$\overline{B_d^0}$ system. The B_s^0-$\overline{B_s^0}$ box diagram is again dominated by t-quark exchange, and the mass difference between the mass eigenstates ΔM_s is given by a formula analogous to that of eq. (36):

$$\Delta M_s = \frac{G_F^2}{6\pi^2} M_W^2 M_{B_s} \left(f_{B_s}^2 \hat{B}_{B_s} \right) \hat{\eta}_{B_s} y_t f_2(y_t) |V_{ts}^* V_{tb}|^2 . \tag{45}$$

Using the fact that $|V_{cb}| = |V_{ts}|$ (eq. 1), it is clear that one of the sides of the unitarity triangle, $|V_{td}/\lambda V_{cb}|$, can be obtained from the ratio of ΔM_d and ΔM_s,

$$\frac{\Delta M_s}{\Delta M_d} = \frac{\hat{\eta}_{B_s} M_{B_s} \left(f_{B_s}^2 \hat{B}_{B_s} \right)}{\hat{\eta}_{B_d} M_{B_d} \left(f_{B_d}^2 \hat{B}_{B_d} \right)} \left| \frac{V_{ts}}{V_{td}} \right|^2 . \tag{46}$$

All dependence on the t-quark mass drops out, leaving the square of the ratio of CKM matrix elements, multiplied by a factor which reflects $SU(3)_{\text{flavour}}$ breaking effects. The only real uncertainty in this factor is the ratio of hadronic matrix elements. Whether or not x_s can be used to help constrain the unitarity triangle will depend crucially on the theoretical status of the ratio $f_{B_s}^2 \hat{B}_{B_s} / f_{B_d}^2 \hat{B}_{B_d}$.

The lattice-QCD results for the hadronic quantities in the B_s system are [51]

$$\hat{B}_{B_s} \simeq \hat{B}_{B_d} = 1.2 \pm 0.2 ,$$

$$\frac{f_{B_s}}{f_{B_d}} = 1.16 \pm 0.1 , \tag{47}$$

while the correspondng values from QCD sum rules are [53]

$$\hat{B}_{B_s} \simeq \hat{B}_{B_d} = 1.0 \pm 0.15 ,$$

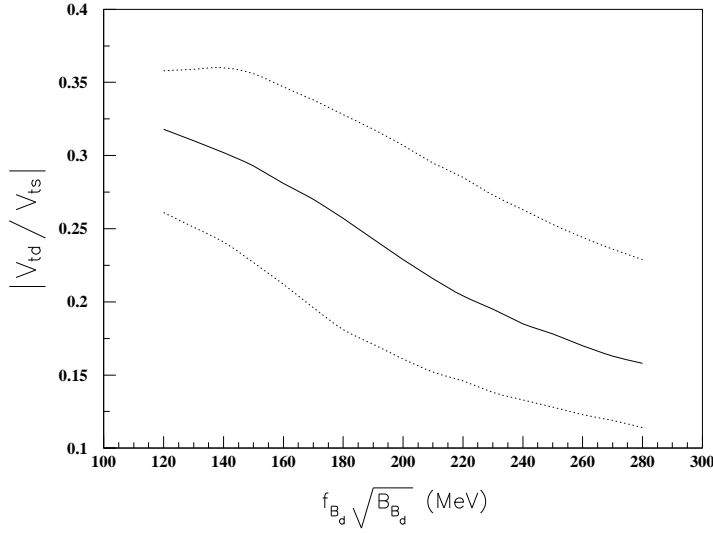$$\frac{f_{B_s}}{f_{B_d}} = 1.16 \pm 0.05 . \tag{48}$$

18

Figure 5: Allowed values of the CKM matrix element ratio $|V_{td}/V_{ts}|$ as a function of the coupling constant product $f_{B_d}\sqrt{\hat{B}_{B_d}}$, for $\hat{B}_K = 0.8\pm0.2$. The solid line corresponds to the best fit values and the dotted curves correspond to the maximum and minimum allowed values at 95 % C.L.

In what follows, we will take $\xi_s \equiv (f_{B_s}\sqrt{\hat{B}_{B_s}})/(f_{B_d}\sqrt{\hat{B}_{B_d}}) = (1.16 \pm 0.1)$. (The SU(3)-breaking factor in $\Delta M_s/\Delta M_d$ is ξ_s^2.)

The mass and lifetime of the B_s meson have now been measured at LEP and Tevatron and their present values are $M_{B_s} = 5368.0 \pm 3.7$ MeV and $\tau(B_s) = 1.54^{+0.14}_{-0.13} \pm 0.05$ ps [57]. We expect the QCD correction factor $\hat{\eta}_{B_s}$ to be equal to its B_d counterpart, i.e. $\hat{\eta}_{B_s} = 0.55$. The main uncertainty in x_s (or, equivalently, ΔM_s) is now $f_{B_s}^2\hat{B}_{B_s}$. Using the determination of A given previously, $\tau_{B_s} = 1.54 \pm 0.14$ (ps) and $\overline{m_t} = 165 \pm 16$ GeV, we obtain

$$x_s = (19.4 \pm 6.9)\frac{f_{B_s}^2\hat{B}_{B_s}}{(230 \text{ MeV})^2} \ . \tag{49}$$

The choice $f_{B_s}\sqrt{\hat{B}_{B_s}} = 230$ MeV corresponds to the central value given by the lattice-QCD estimates, and with this our fits give $x_s \simeq 20$ as the preferred value in the SM. Allowing the coefficient to vary by $\pm 2\sigma$, and taking the central value for $f_{B_s}\sqrt{\hat{B}_{B_s}}$, this gives

$$5.6 \leq x_s \leq 33.2 \ . \tag{50}$$

It is difficult to ascribe a confidence level to this range due to the dependence on the unknown coupling constant factor. All one can say is that the standard model predicts large values for x_s, most of which are above the present experimental limits.

An alternative estimate of ΔM_s (or x_s) can also be obtained by using the relation in eq. (46). Two quantities are required. First, we need the CKM ratio $|V_{ts}/V_{td}|$. In Fig. 5 we show the allowed values (at 95% C.L.) of the inverse of this ratio as a function of $f_{B_d}\sqrt{\hat{B}_{B_d}}$, for $\hat{B}_K = 0.8 \pm 0.2$. From this one gets

$$2.76 \leq \left|\frac{V_{ts}}{V_{td}}\right| \leq 8.4 \ . \tag{51}$$

The second ingredient is the SU(3)-breaking factor which we take to be $\xi_s = 1.16 \pm 0.1$, or $1.1 \leq \xi_s^2 \leq 1.6$. The result of the CKM fit can therefore be expressed as a 95% C.L.
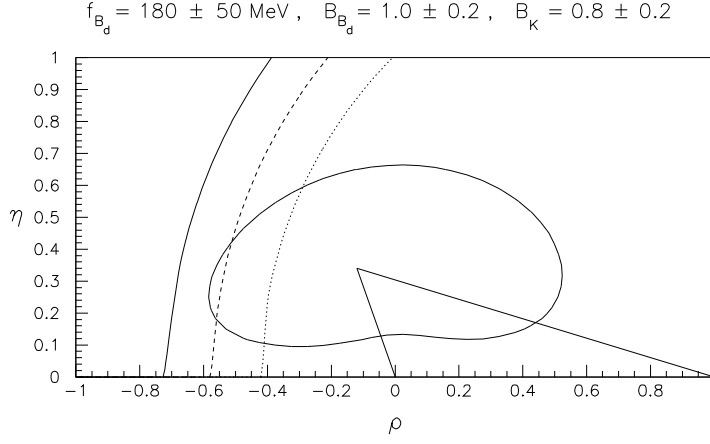
19

$f_{B_d} = 180 \pm 50$ MeV , $B_{B_d} = 1.0 \pm 0.2$, $B_K = 0.8 \pm 0.2$

Figure 6: Further constraints in ρ-η space from the ALEPH bound on ΔM_s. The bounds are presented for 3 choices of the SU(3)-breaking parameter: $\xi_s = 1.1$ (dotted line), 1.35 (dashed line) and 1.6 (solid line). In all cases, the region to the left of the curve is ruled out.

range:

$$10.3 \left(\frac{\xi_s}{1.16} \right)^2 \;\; \leq \;\; \frac{\Delta M_s}{\Delta M_d} \;\; \leq \;\; 94.9 \left(\frac{\xi_s}{1.16} \right)^2 . \tag{52}$$

Again, it is difficult to assign a true confidence level to $\Delta M_s / \Delta M_d$ due to the dependence on ξ_s. The large allowed range reflects our poor knowledge of the matrix element ratio $|V_{ts}/V_{td}|$, which shows that this method is not particularly advantageous at present for the determination of the range for ΔM_s.

The ALEPH lower bound $\Delta M_s / \Delta M_d > 11.3$ at 95% C.L. can be turned into a bound on the CKM parameter space (ρ, η) by choosing a value for the SU(3)-breaking parameter ξ_s^2. We assume three representative values: $\xi_s^2 = 1.1$, 1.35 and 1.6, and display the resulting constraints in Fig. 6. From this graph we see that the ALEPH bound marginally restricts the allowed ρ-η region for small values of ξ_s^2, but does not provide any useful bounds for larger values.

Summarizing the discussion on x_s, we note that the lattice-QCD-inspired estimate $f_{B_s} \sqrt{\hat{B}_{B_s}} \simeq 230$ MeV and the CKM fit predict that x_s lies between 6 and 33, with a central value around 20. The upper and lower bounds and the central value scale as $(f_{B_s} \sqrt{\hat{B}_{B_s}}/230 \text{ MeV})^2$. The present constraints from the lower bound on x_s on the CKM parameters are marginal but this would change with improved data. Of course, an actual measurement of x_s would be very helpful in further constraining the CKM parameter space.

5 CP Violation in the B System

It is expected that the B system will exhibit large CP-violating effects, characterized by nonzero values of the angles α, β and γ in the unitarity triangle (Fig. 1) [55]. These angles can be measured via CP-violating asymmetries in hadronic B decays. In the decays $\overset{(-)}{B_d} \to \pi^+ \pi^-$, for example, one measures the quantity $\sin 2\alpha$, and in $\overset{(-)}{B_d} \to J/\psi K_S$, $\sin 2\beta$ is obtained. The CP asymmetry in the decay $\overset{(-)}{B_s} \to D_s^\pm K^\mp$ is slightly different, yielding $\sin^2 \gamma$.

These CP-violating asymmetries can be expressed straightforwardly in terms of the CKM parameters ρ and η. The 95% C.L. constraints on ρ and η found previously can

$f_{B_d}\sqrt{\hat{B}_{B_d}}$ (MeV)	$\sin 2\alpha$	$\sin 2\beta$	$\sin^2 \gamma$
130	$0.36 - 0.96$	$0.17 - 0.41$	$0.08 - 0.48$
155	$0.15 - 1.0$	$0.26 - 0.62$	$0.23 - 1.0$
180	$-1.0 - 1.0$	$0.33 - 0.81$	$0.37 - 1.0$
205	$-1.0 - 1.0$	$0.40 - 0.93$	$0.20 - 1.0$
230	$-1.0 - 0.86$	$0.47 - 0.99$	$0.15 - 1.0$

Table 6: The allowed ranges for the CP asymmetries $\sin 2\alpha$, $\sin 2\beta$ and $\sin^2 \gamma$, corresponding to the constraints on ρ and η shown in Fig. 2. Values of the coupling constant $f_{B_d}\sqrt{\hat{B}_{B_d}}$ are stated. We fix $\hat{B}_K = 0.8$. The range for $\sin 2\beta$ includes an additional minus sign due to the CP of the final state $J/\Psi K_S$.

be used to predict the ranges of $\sin 2\alpha$, $\sin 2\beta$ and $\sin^2 \gamma$ allowed in the standard model. The allowed ranges which correspond to each of the figures in Fig. 2, obtained from Fit 1, are found in Table 6. In this Table we have assumed that the angle β is measured in $\overset{(-)}{B_d} \to J/\Psi K_S$, and have therefore included the extra minus sign due to the CP of the final state.

Since the CP asymmetries all depend on ρ and η, the ranges for $\sin 2\alpha$, $\sin 2\beta$ and $\sin^2 \gamma$ shown in Table 6 are correlated. That is, not all values in the ranges are allowed simultaneously. We illustrate this in Fig. 7, corresponding to the "experimental fit" (Fit 1), by showing the region in $\sin 2\alpha$-$\sin 2\beta$ space allowed by the data, for various values of $f_{B_d}\sqrt{\hat{B}_{B_d}}$. Given a value for $f_{B_d}\sqrt{\hat{B}_{B_d}}$, the CP asymmetries are fairly constrained. However, since there is still considerable uncertainty in the values of the coupling constants, a more reliable profile of the CP asymmetries at present is given by our "combined fit" (Fit 2), where we convolute the present theoretical and experimental values in their allowed ranges. The resulting correlation is shown in Fig. 8. From this figure one sees that the smallest value of $\sin 2\beta$ occurs in a small region of parameter space around $\sin 2\alpha \simeq 0.4$-0.6. Excluding this small tail, one expects the CP-asymmetry in $\overset{(-)}{B_d} \to J/\Psi K_S$ to be at least 30%.

6 Summary and Outlook

We summarize our results:

(i) We have presented an update of the CKM unitarity triangle following from the additional experimental input of $m_t = 174 \pm 16$ GeV [1]. The fits can be used to exclude extreme values of the pseudoscalar coupling constants, with the range 110 MeV $\leq$ $f_{B_d}\sqrt{\hat{B}_{B_d}} \leq 290$ MeV still allowed for $\hat{B}_K = 1$. The lower limit of this range is quite $\hat{B}_K$-independent, but the upper limit is strongly correlated with the value chosen for $\hat{B}_K$. For example, for $\hat{B}_K = 0.8$, 0.6 and 0.4, $f_{B_d}\sqrt{\hat{B}_{B_d}} \leq 270$, 230 and 180 MeV, respectively, is required for a good fit. The solutions for $\hat{B}_K = 0.8 \pm 0.2$ are slightly favoured by the data as compared to the lower values. These numbers are in very comfortable agreement with QCD-based estimates from sum rules and lattice techniques. The statistical significance
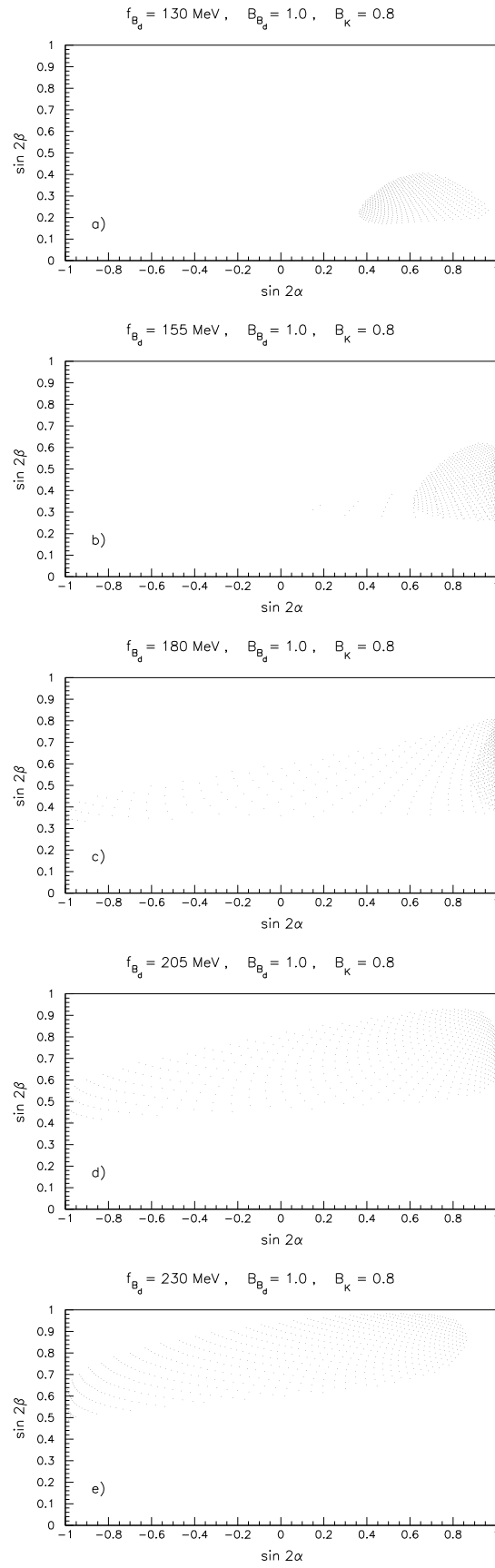
21

Figure 7: Allowed region of the CP asymmetries $\sin 2\alpha$ and $\sin 2\beta$ resulting from the "experimental fit" of the data for different values of the coupling constant $f_{B_d}\sqrt{\hat{B}_{B_d}}$ indicated on the figures a) – e). We fix $\hat{B}_K = 0.8$.
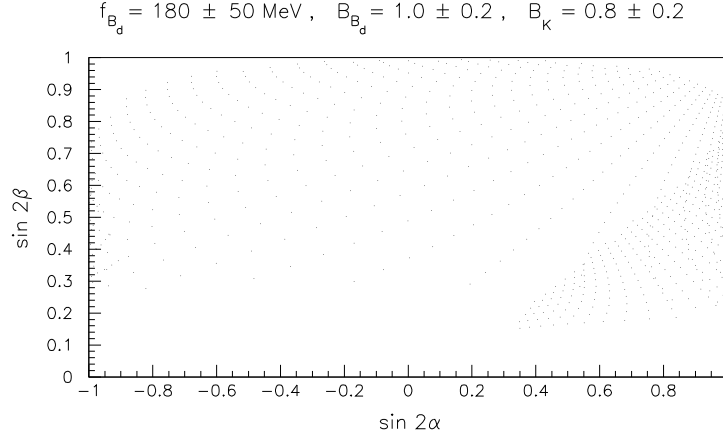
$$f_{B_d} = 180 \pm 50 \text{ MeV} , \quad B_{B_d} = 1.0 \pm 0.2 , \quad B_K = 0.8 \pm 0.2$$

Figure 8: Allowed region of the CP asymmetries $\sin 2\alpha$ and $\sin 2\beta$ resulting from the "combined fit" of the data for the ranges for $f_{B_d}\sqrt{\hat{B}_{B_d}}$ and $\hat{B}_K$ given in the text.

of the fit is, however, not good enough to determine the coupling constant more precisely. We note that the quality of fit for $\hat{B}_K \leq 0.4$ is generally poor.

(ii) The allowed CKM unitarity triangle in the (ρ, η)-space is more restricted than obtained previously without the top quark mass input. However, the present uncertainties are still enormous – despite the new, more accurate experimental data, our knowledge of the unitarity triangle is still poor. This underscores the importance of measuring CP-violating rate asymmetries in the B system. Such asymmetries are largely independent of theoretical hadronic uncertainties, so that their measurement will allow us to accurately pin down the parameters of the CKM matrix. Furthermore, unless our knowledge of the pseudoscalar coupling constants improves considerably, better measurements of such quantities as x_d will not help much in constraining the unitarity triangle. On this point, help may come from the experimental front. It may be possible to measure the parameter f_{B_d}, using isospin symmetry, via the charged-current decay $B_u^\pm \to \tau^\pm \nu_\tau$. With $|V_{ub}/V_{cb}| = 0.08 \pm 0.03$ and $f_{B_d} = 180 \pm 50$ MeV, one gets a branching ratio $BR(B_u^\pm \to \tau^\pm \nu_\tau) = (0.1$–$1.7) \times 10^{-4}$, with $BR(B_u^\pm \to \tau^\pm \nu_\tau) = 5.2 \times 10^{-5}$ as the central value. This lies in the range of the future LEP and asymmetric B-factory experiments, though at LEP the rate $Z \to B_c X \to \tau^\pm \nu_\tau X$ could be just as large as $Z \to B^\pm X \to \tau^\pm \nu_\tau X$. Along the same lines, the prospects for measuring (f_{B_d}, f_{B_s}) in the FCNC leptonic and photonic decays of B_d^0 and B_s^0 hadrons, $(B_d^0, B_s^0) \to \mu^+ \mu^-, (B_d^0, B_s^0) \to \gamma\gamma$ in future B physics facilities are not entirely dismal [58].

(iii) We have determined bounds on the ratio $|V_{td}/V_{ts}|$ from our fits. For 110 MeV $\leq f_{B_d}\sqrt{\hat{B}_{B_d}} \leq 290$ MeV, i.e. in the entire allowed domain, at 95 % C.L. we find

$$0.11 \leq \left| \frac{V_{td}}{V_{ts}} \right| \leq 0.36 . \tag{53}$$

The upper bound from our analysis is more restrictive than the current experimental upper limit following from the CKM-suppressed radiative penguin decays $BR(B \to \omega + \gamma)$ and $BR(B \to \rho + \gamma)$, which at present yield at 90% C.L. [59]

$$\left| \frac{V_{td}}{V_{ts}} \right| \leq 0.64 - 0.75 , \tag{54}$$

depending on the model used for the SU(3)-breaking in the relevant form factors [60]. Furthermore, the upper bound is now as good as that obtained from unitarity, which gives $0.08 \leq |V_{td}/V_{ts}| \leq 0.36$ [61], but the lower bound from our fit is more restrictive.

Note that the matrix element ratio $|V_{ub}/V_{cb}|$ is very poorly determined. Our fits give:

$$0.03 \leq \frac{|V_{ub}|}{|V_{cb}|} \leq 0.137 \ , \tag{55}$$

It is important to reduce the present errors on this ratio. In particular, a better determination of $|V_{ub}/V_{cb}|$ should be put as a high priority item on the agenda of the ongoing experiments at CLEO and LEP. We note here that the relations between the exclusive and inclusive decays involving $b \to u\ell\nu_\ell$ and $b \to s\gamma$ transitions, which have been discussed using the HQET methods, can be used to relate $|V_{ub}|$ to $|V_{ts}| = |V_{cb}|$.

(iv) Using the measured value of m_t, we find

$$x_s = (19.4 \pm 6.9) \frac{f_{B_s}^2 \hat{B}_{B_s}}{(230 \text{ MeV})^2} \ . \tag{56}$$

Taking $f_{B_s}\sqrt{\hat{B}_{B_s}} = 230$ (the central value of lattice-QCD estimates), and allowing the coefficient to vary by $\pm 2\sigma$, this gives

$$5.6 \leq x_s \leq 33.2 \ . \tag{57}$$

No reliable confidence level can be assigned to this range – all that one can conclude is that the SM predicts large values for x_s, most of which lie above the ALEPH 95% C.L. lower limit of $x_s > 9.0$.

(v) The ranges for the CP-violating rate asymmetries parametrized by $\sin 2\alpha$, $\sin 2\beta$ and and $\sin^2 \gamma$ are determined at 95% C.L. to be

$$\begin{aligned}
-1.0 &\leq \sin 2\alpha \leq 1.0 \ , \\
0.17 &\leq \sin 2\beta \leq 0.99 \ , \\
0.08 &\leq \sin^2 \gamma \leq 1.0 \ .
\end{aligned} \tag{58}$$

(For $\sin 2\alpha < 0.4$, we find $\sin 2\beta \geq 0.3$.)

Acknowledgements:

References

[1] F. Abe et al. (CDF Collaboration) FERMILAB-PUB-94/097-E; FERMILAB-PUB-94/116-E.

[2] The LEP Collaborations ALEPH, DELPHI, L3 and OPAL and the LEP Electroweak Working Group, Preprint LEPEWWG/94-102 (1994);
D. Schaile, Rapporteur talk, 27th International Conference on High Energy Physics ICHEP94, Glasgow, July 20-27, 1994.

[3] F. Abachi et al. (D0 Collaboration), Phys. Rev. Lett. **72** (1994) 2138;
P. Grannis, Rapporteur talk, ICHEP94, Glasgow, July 20-27, 1994.

[4] S.L. Glashow, Nucl. Phys. **22** (1961) 579; A. Salam in Elementary Particle Theory, ed. N. Svartholm (Almqvist and Wiksell, Stockholm, 1968); S. Weinberg, Phys. Rev. Lett. **19** (1967) 1264.

[5] N. Cabibbo, Phys. Rev. Lett. **10** (1963) 531; M. Kobayashi and T. Maskawa, Prog. Theor. Phys. **49** (1973) 652.

[6] See, for example, A.J. Buras and M.K. Harlander in *Heavy Flavours*, A.J. Buras and M. Lindner (eds.), Advanced Series on Directions in High Energy Physics (World Scientific, Singapore, 1992), Vol. 10.

[7] A. Ali and D. London, CERN-TH.7248/94 (unpublished).

[8] A. Pich and J. Prades, Valencia report FTUVC/94-37, IFIC/94-32, NBI-94/32 (1994).

[9] W. de Boer, R. Ehret and S. Schael, Univ. of Karlsruhe report IEKP-KA/94-09 (1994).

[10] A.J. Buras, M.E. Lautenbacher and G. Ostermaier, Max-Planck-Institute report MPI-Ph/94-14 (1994).

[11] N. Gray, D.J. Broadhurst, W. Grafe and K. Schilcher, Z. Phys. **C48** (1990) 673.

[12] We thank A. Pich for pointing this out to us.

[13] B. Barish et al. (CLEO Collaboration), Preprint CLNS 94/1285 (1994).

[14] H. Albrecht et al. (ARGUS Collaboration), Phys. Lett. **B324** (1994) 249; H. Schröder (private communication).

[15] D. Buskulic et al. (ALEPH Collaboration), submitted paper to the International Conference on High Energy Physics, Glasgow, ICHEP94-0605 (1994).

[16] M. Neubert, preprint CERN-TH.7395/94 (1994).

[17] M. Shifman, N.G. Uraltsev and A. Vainshtain, Preprint TPI-MINN-94/13-T (1994).

[18] R. Forty, Rapporteur talk, ICHEP94, Glasgow, July 20 – 27, 1994.

[19] Y. Pan (ALEPH Collaboration), talk presented in the parallel session PA-9b, ICHEP94, Glasgow, July 20 – 27, 1994.

[20] L. Wolfenstein, Phys. Rev. Lett. **51** (1983) 1945.

[21] K. Hikasa et al. (Particle Data Group), Phys. Rev. **D45** (1992) 1.

[22] N. Isgur and M. Wise, Phys. Lett. **B232** (1989) 113; **B237** (1990) 527.

[23] M.E. Luke, Phys. Lett. **B252** (1990) 447.

[24] C.G. Boyd and D.E. Brahm, Phys. Lett. **B257** (1991) 393.

[25] M. Neubert and V. Rieckert, Nucl. Phys. **B382** (1992) 97; M. Neubert, Phys. Lett. **B264** (1991) 455, Phys. Rev. **D46** (1992) 2212.

[26] M.B. Voloshin and M.A. Shifman, Sov. J. Nucl. Phys. **45** (1987) 292.

[27] M. Neubert, CERN-TH.7255/94 (1994); to appear in the Proceedings of TASI-93, Boulder, Colorado, 1993.

[28] T. Mannel, Phys. Rev. **D50** (1994) 428.

[29] P. Ball and V. Braun, Phys. Rev. **D49** (1994) 2472.

[30] H. Albrecht et al. (ARGUS Collaboration), Phys. Lett. **B275** (1992) 195; Z. Phys. **C57** (1993) 533.

[31] P. Avery et al. (CLEO Collaboration), Preprint CLEO CONF 94-7 (1994).

[32] J.D. Bjorken, in Gauge Bosons and Heavy Quarks, Proceedings of 18th SLAC Summer Institute on Particle Physics, Stanford, California, 1990, ed. J.F. Hawthorne (SLAC Report No. 378, Stanford, 1991).

[33] M.B. Voloshin, Phys. Rev. **D46** (1992) 3062.

[34] D. Cassel (private communication).

[35] R. Patterson, Rapporteur talk, ICHEP94, Glasgow, July 20-27, 1994.

[36] S.P. Booth et al. (UKQCD Collaboration), Phys. Rev. Lett. **72** (1994) 462.

[37] A. Soni (in CP Workshop, Technion, Haifa, June 7 - 9, 1994).

[38] C. Bernard, Y. Shen and A. Soni, Phys. Lett. **B317** (1993) 164.

[39] S. Narison, Preprint CERN-TH.7277/94 (1994).

[40] M. Luke and M.J. Savage, Phys. Lett. **321** (1994) 88.

[41] P. Ball and U. Nierste, TU München Preprint TUM-T31-56/94/R (1994).

[42] H. Albrecht et al. (ARGUS Collaboration), Phys. Lett. **B234** (1991) 297.

[43] R. Fulton et al. (CLEO Collaboration), Phys. Rev. Lett. **64** (1990) 16.

[44] J. Bartelt et al. (CLEO Collaboration), Phys. Rev. Lett. **71** (1993) 4111.

[45] A.J. Buras, W. Słominski and H. Steger, Nucl. Phys. **B238** (1984) 529; **B245** (1984) 369.

[46] S. Herrlich and U. Nierste, Nucl. Phys. **B419** (1994) 292.

[47] A.J. Buras, M. Jamin and P.H. Weisz, Nucl. Phys. **B347** (1990) 491.

[48] J. Flynn, Mod. Phys. Lett. **A5** (1990) 877.

[49] T. Inami and C.S. Lim, Prog. Theor. Phys. **65** (1981) 297.

[50] A. Ali and D. London, J. Phys. G: Nucl. Part. Phys. **19** (1993) 1069.

[51] J. Shigemitsu, Rapporteur talk, ICHEP94, Glasgow, July 20 – 27, 1994.

[52] M.B. Gavela et al., Phys. Lett. **B206** (1988) 113; Nucl. Phys. **B306** (1988) 677;
C. Bernard and A. Soni, Nucl. Phys. B (Proc. Suppl.) **17** (1990) 495;
G.W. Kilcup, S.R. Sharpe, R. Gupta and A. Patel, Phys. Rev. Lett. **64** (1990) 25;
R. Gupta et al., Phys. Rev. **D47** (1993) 5113;
S.R. Sharpe, Nucl. Phys. B (Proc. Suppl.) **34** (1994) 403.

[53] S. Narison, Phys. Lett. **B 322** (1994) 247;
S. Narison and A. Pivovarov, Phys. Lett. **B327** (1994) 341.

[54] R. Sommer, DESY Report 94-011 (1994).

[55] For reviews, see, for example, Y. Nir and H.R. Quinn in "B Decays," ed. S. Stone (World Scientific, Singapore, 1992), p. 362; I. Dunietz, *ibid* p. 393.

[56] R. Aleksan, B. Kayser and D. London, Phys. Rev. Lett. **73** (1994) 18.

[57] P. Roudeau, Rapporteur talk, ICHEP94, Glasgow, July 20 – 27, 1994.

[58] A. Ali in "B Decays" (2. Edition), ed. S. Stone (World Scientific, Singapore, 1994).

[59] M. Athanas et al. (CLEO Collaboration), CLEO CONF 94-2 (1994).

[60] A. Ali, V.M. Braun and H. Simma, CERN TH.7118/93 (1993);
J.M. Soares, Phys. Rev. D49 (1994) 283;
S. Narison, Phys. Lett. B327 (1994) 354.

[61] We thank Y. Nir for a discussion of this point.